J. Fluid Mech. (1965), *vol.* 23, *part* 1, *pp.* 185–208
Printed in Great Britain

Calibration of the Preston tube and limitations on its use in pressure gradients

By V. C. PATEL

Engineering Laboratory, Cambridge University

(Received 5 November 1964 and in revised form 21 December 1964)

Preston's method of measuring skin friction in the turbulent boundary layer makes use of a circular Pitot tube resting on the wall. On the assumption of a velocity distribution in the wall region common to boundary layer and pipe flows the calibration curve for the Pitot tube can be obtained in fully developed pipe flow. Earlier experiments suggested that Preston's original calibration was in error, and a revised calibration curve has been obtained and is presented here.

From experiments in strong favourable and adverse pressure gradients, limits are assigned to the pressure-gradient conditions within which the calibration can be used with prescribed accuracy. It is shown that in sufficiently strong favourable gradients the 'inner-law' velocity distribution breaks down completely, and it is suggested that this breakdown is associated with reversion to laminar flow.

As an incidental result, values have been obtained for the constants occurring in the logarithmic expression for the inner-law velocity distribution.

1. Introduction

Preston's method of measuring turbulent skin friction, which makes use of a simple Pitot tube resting on the surface (the so-called Preston tube), depends upon the assumption of a universal inner law (or law of the wall) common to boundary layers and fully developed pipe flow. The difference between the pressure recorded by the Preston tube and the undisturbed static pressure can then be expressed in the non-dimensional, form

$$\Delta p_p/\rho U_\tau^2 = \mathrm{f}(U_\tau d/\nu),$$

where Δp_p is the Preston tube reading (i.e. the difference between Pitot and static pressures), d is the diameter of the Preston tube, and $U_\tau \equiv (\tau_0/\rho)^{\frac{1}{2}}$ is the friction velocity. ρ and ν are the fluid density and kinematic viscosity respectively, and τ_0 the wall-shear stress.

Alternatively, the non-dimensional relationship between Preston-tube reading and skin friction can be presented in the practically more convenient form given by Preston (1954), namely,

$$\frac{\tau_0 d^2}{4\rho\nu^2} = \mathrm{F}\left(\frac{\Delta p_p d^2}{4\rho\nu^2}\right)$$

and the function F can readily be determined from measurements in fully developed pipe flow.

Experimental evidence obtained at the National Physical Laboratory by Bradshaw & Gregory (1958) and others and in America by Smith & Walker (1958) cast considerable doubt on the assumption of a universal inner law common to fully developed pipe flow and flat-plate boundary layers, but subsequent experiments by Head & Rechenberg (1962) provided convincing evidence for the correctness of the assumption, and the soundness of Preston's method of measuring skin friction. The experiments also suggested, however, that Preston's original calibration was somewhat in error, and the main object of the present paper is to present what, it is hoped, can be regarded as a definitive calibration curve for the Preston tube and, in addition, to assign experimentally-determined limits to the pressure-gradient conditions within which the calibration remains valid. One surprising result of the investigation is that favourable pressure-gradient conditions are rather more critical than similar adverse gradients. It seems likely that this breakdown of the inner law in sufficiently strong favourable pressure gradients is associated with reversion of the turbulent boundary layer to laminar flow, a phenomenon which has been mentioned in the literature but not extensively explored.

As an incidental result of the investigation, values have been obtained for the constants A and B appearing in the logarithmic region of the inner-law velocity distribution.

2. Calibration experiments

Three different pipes with nominal bores of 8 in., 2 in. and $\frac{1}{2}$ in. were used in calibrating the Preston tubes. A detailed description of the 8 in. pipe has been given by Head & Rechenberg (1962) and that of the 2 in. pipe by Preston (1954).

Tube no.	external diameter d (in.)	Approx. diameter ratio	stem centre line to mouth distance (in.)	where used (pipe diameter, in.)
1	0·498	0·6	2	8
2	0·375	0·6	2	8
3(A)	0·249	0·6	2	8, 2
4	0·187	0·6	2	8
5	0·1205	0·6	2	8, 2
6	0·090	0·6	2	8, 2
7	0·054	0·6	2	8, 2
8	0·0285	0·6	2	8, 2
9	0·0235	0·6	2	8, 2
1A	0·250	0·83	2	8, 2
2A	0·2495	0·38	2	8
3A	0·2495	0·17	2	8
1B	0·0420	0·6	1	$\frac{1}{2}$
2B	0·0260	0·6	1	$\frac{1}{2}$

TABLE 1. Details of Preston tubes.

The $\frac{1}{2}$ in. diameter pipe was made up of long sections of drawn brass tubing. Constructional details of Preston tubes are given in the above references, and additional information is presented in table 1. The distances from entry to the first measuring station in the 8 in., 2 in., and $\frac{1}{2}$ in. pipes were respectively 72, 90 and 320 diameters. The skin friction was computed from the pressure drop along the pipe downstream of the first station.

8 in. diameter pipe

Preliminary experiments showed some disagreement with the calibration results of Head & Rechenberg, even though the apparatus used was basically the same. The source of this discrepancy was traced to misalignment of the flange joints between adjacent sections of the pipe which was found to cause circumferential variations of up to 4 % in static pressure. To eliminate the necessity for disconnecting the working section whenever a different Preston tube was inserted, brass plugs were fitted at two positions about 6 diameters apart in the streamwise direction so that Preston tubes up to $\frac{1}{2}$ in. diameter could be fitted without disturbing the alignment of the flanges. The final location of the various sections of the pipe was determined by ensuring a linear fall in pressure along the pipe, the flange alignment being adjusted at the same time until four identical surface Pitots (diameter 0·250 in.) equally spaced around the circumference gave the same reading. This procedure reduced the circumferential variation in static pressure to less than 1 % of the centre-line dynamic pressure. Preston-tube readings at the two positions were in excellent agreement, and velocity profiles measured at these stations (by means of a flattened Pitot) also agreed closely.

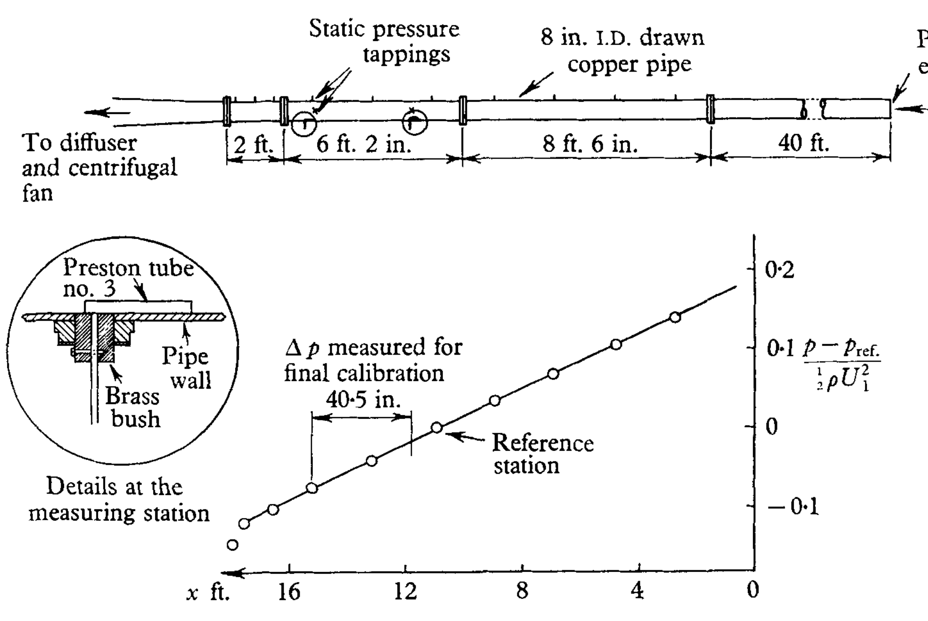

FIGURE 1. Calibration of Preston tubes in 8 in. diameter pipe.

The general arrangement of the apparatus with details of the brass plugs and location of the flange joints, and the pressure distribution along the 8 in. pipe are shown in figure 1. A typical velocity profile plotted in the semi-logarithmic form is shown in figure 2. From these measurements it was concluded that the flow was fully developed and axially symmetric.

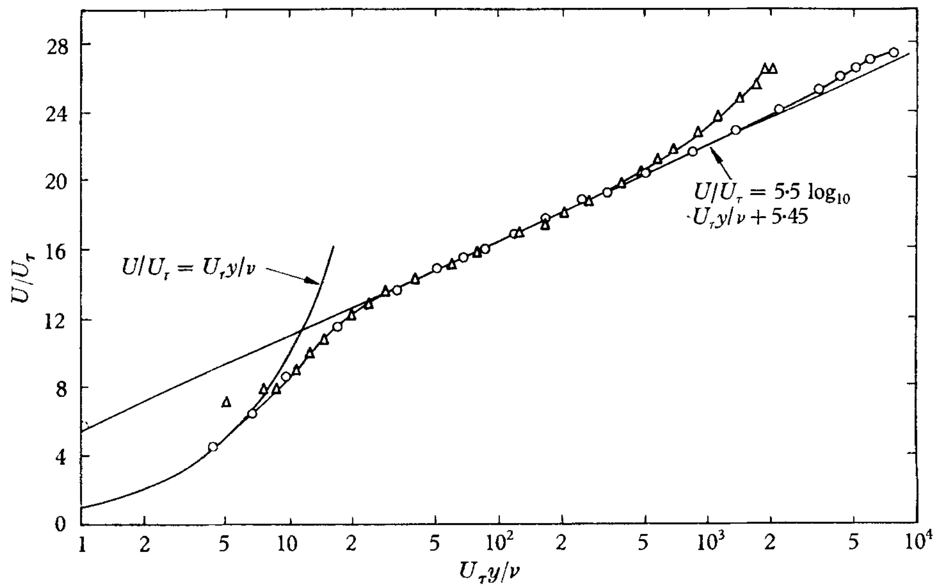

FIGURE 2. Comparison of velocity profiles in pipe flow and zero-pressure-gradient boundary layer. ○, Fully developed pipe flow, 8 in. diameter pipe; △, flat plate (zero pressure gradient) boundary layer (flattened Pitot results).

For the final calibration, static pressures were measured over a test length of 40·5 in. (see figure 1) by tappings in the wall at the upstream end and a 0·040 in. static probe located on the centre-line of the pipe at the downstream end. Care was taken to ensure that the surface of the pipe between the two positions was smooth. The Preston-tube reading and corresponding static-pressure drop were then recorded for various air speeds. The static pressures at the measuring station, with and without the Preston tube in position, were also noted. This procedure was repeated for the tubes listed in table 1. The ranges of Reynolds number covered by these measurements were

$$7{\cdot}9\times 10^4 < U_1 D/\nu < 6{\cdot}15\times 10^5,$$

and

$$12 < U_\tau d/\nu < 1270,$$

where U_1 is the maximum velocity in the pipe, D is the diameter of the pipe and d is the diameter of the Preston tube.

2 in. diameter pipe

The calibration in this case was relatively simple since the pipe was in one straight length and Preston's original experimental arrangement was simply reproduced. The effect of the Preston tube on the local static pressure was appreciably larger than for the corresponding case (i.e. the same ratio d/D) in the 8 in. pipe. This result, which did not of course affect the accuracy of the final calibration, was due to the lack of complete geometrical similarity between the Preston tubes (see figure 3) since the same tubes were used in the two pipes. For these tests,

$$1{\cdot}6 \times 10^4 < U_1 D/\nu < 1{\cdot}3 \times 10^5,$$

and

$$9 < U_\tau d/\nu < 695.$$

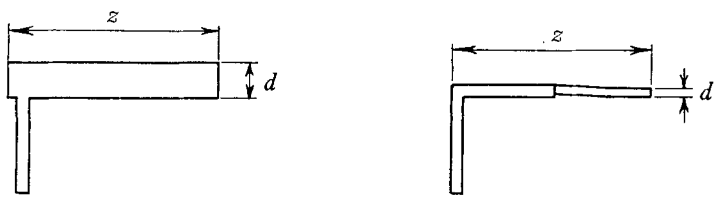

Preston tube 2 in. 8 in. pipe
$d = 0{\cdot}375$ in.
$D = 8{\cdot}00$ in.
$d/D = 0{\cdot}047$
$z/D = 0{\cdot}272$

Preston tube 6 in 2 in. pipe
$d = 0{\cdot}090$ in.
$D = 2{\cdot}00$ in.
$d/D = 0{\cdot}045$
$z/D = 1{\cdot}03$

FIGURE 3. Illustration of the lack of complete geometrical similarity in Preston tubes at the same d/D ratio.

½ in. diameter pipe

The pressure drop in the ½ in. diameter pipe was measured over a length of 100 diameters. The results presented here are those for which compressibility corrections were negligible. At higher speeds it was found that attempts to apply approximate corrections did not lead to consistent results and readings for these conditions have therefore not been used. The Reynolds-number ranges covered in these experiments were

$$8{\cdot}3 \times 10^3 < U_1 D/\nu < 2{\cdot}6 \times 10^4 \text{ (approx.)},$$

and

$$24 < U_\tau d/\nu < 140.$$

Corrections

The values used for ρ and ν were those corresponding to stream temperature and pressure at the measuring station. Two major blockage corrections were applied to the measurements. These take account of the effects of the presence of the Preston tube on (*a*) the measured pressure drop and (*b*) the tube reading itself, due to the change in the local static pressure. These corrections therefore allow for the lack of geometrical similarity of Preston tubes. Compressibility corrections in the experiments reported here were less than 1 % of τ_0.

3. Results

The experimental calibration curve has been plotted in figure 4 in the form suggested by Preston, i.e.

$$\frac{\tau_0 d^2}{4\rho\nu^2} = \mathrm{F}\left(\frac{\Delta p_p d^2}{4\rho\nu^2}\right). \tag{1}$$

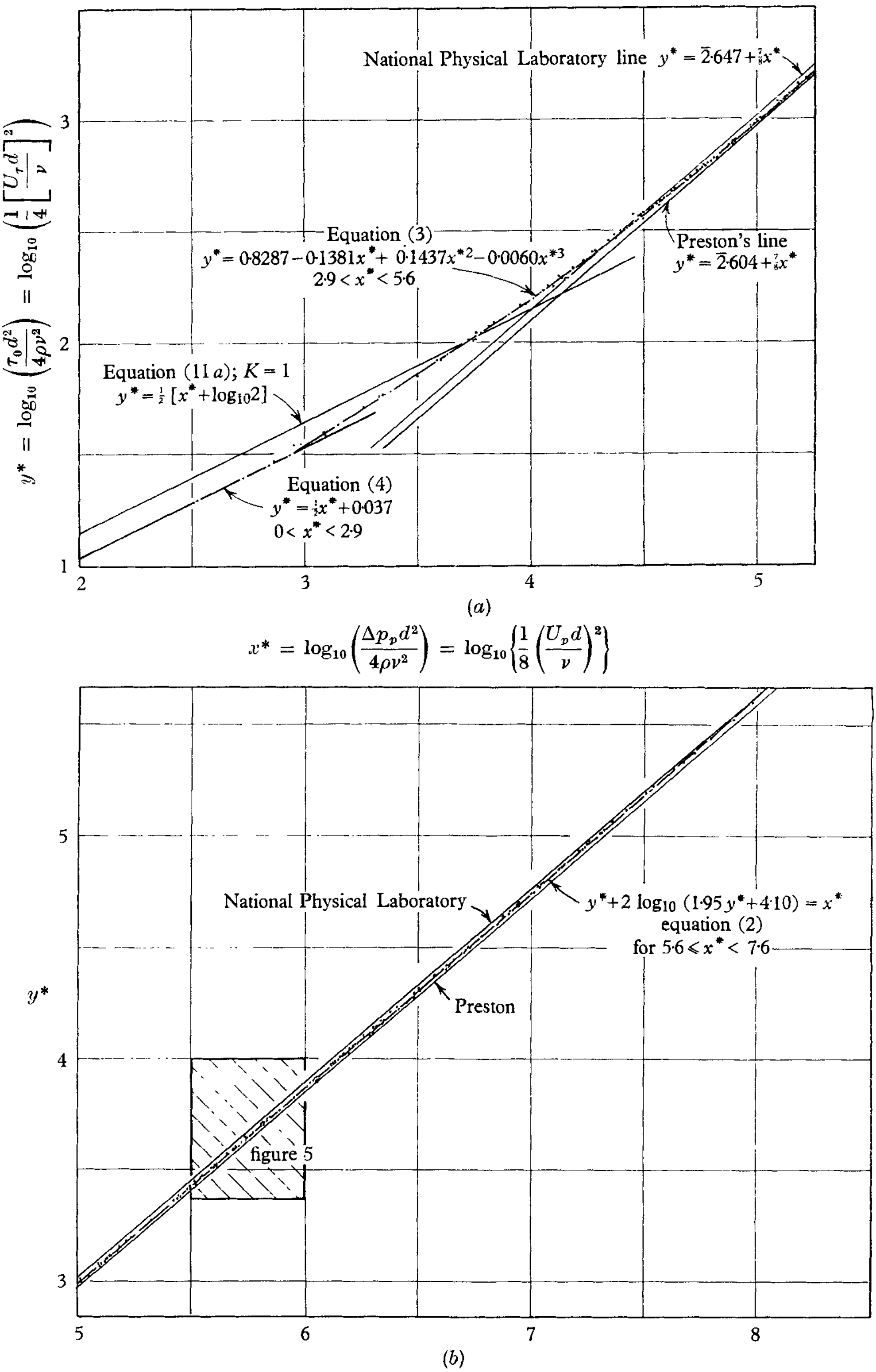

FIGURE 4. Calibration of Preston tubes in 8, 2 and $\frac{1}{2}$ in. diameter pipes.

Owing to the large number of experimental points and the small scale to which the figure is reproduced, no attempt has been made to distinguish the results from different pipes or different Preston tubes in this figure, but a small portion of the calibration curve has been reproduced in figure 5 on a larger scale to show the

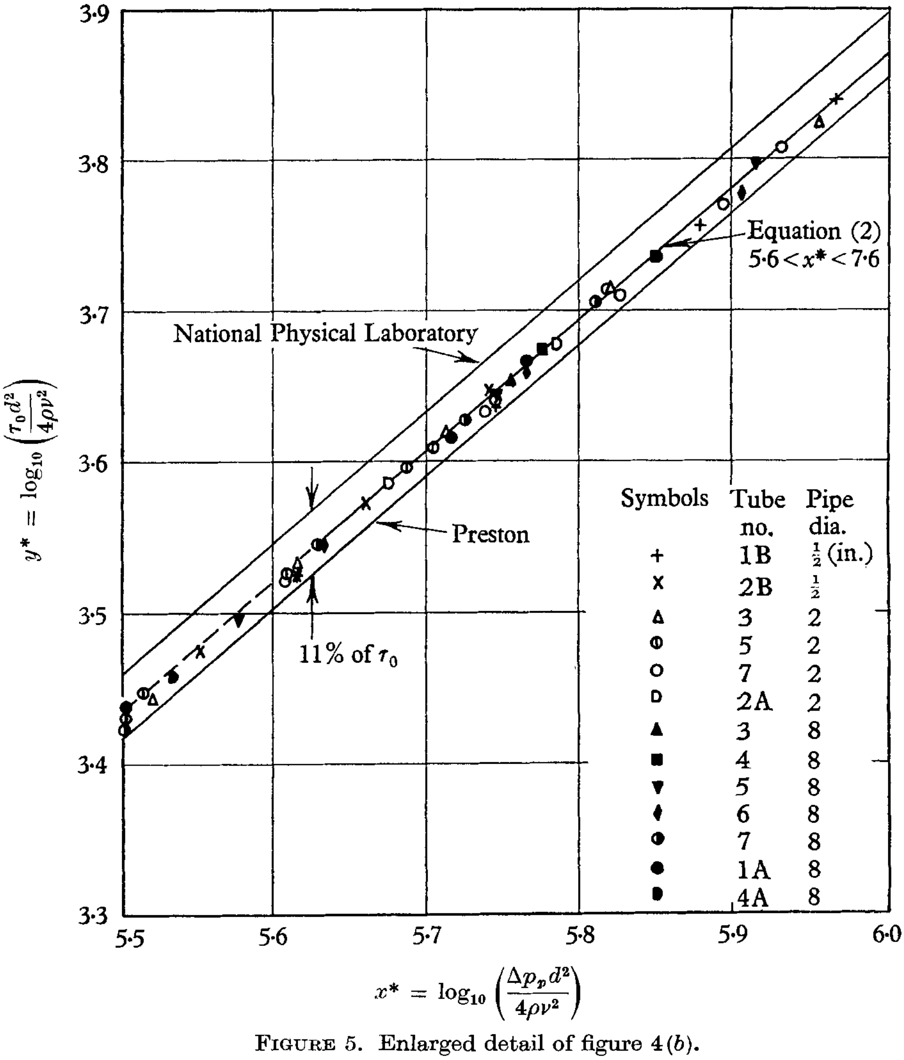

FIGURE 5. Enlarged detail of figure 4(*b*).

general level of agreement of the experimental results. The expressions quoted by Preston (1954) and the staff of the National Physical Laboratory (1958) are also included for comparison. It is seen that the calibration in the three pipes agrees closely, and also that the results from various tubes fall on a single curve. This implies that F is unique and the law of the wall is identical in the three pipes.

The calibration, in the range

$$3{\cdot}5 < \log_{10}\left(\frac{\tau_0 d^2}{4\rho\nu^2}\right) < 5{\cdot}3,$$

i.e.
$$55 < U_\tau d/(2\nu) < 800,$$

is not found to be a straight line as suggested by Preston and other experimenters, but is a curve giving values of τ_0 some 3 % higher than Preston's at the lower limit and about 9 % higher at the upper limit. This divergence was noted by Head & Rechenberg and their results are in excellent agreement with the present ones. In the above range, a curve which fits the experimental calibration within ± 1 % of τ_0 is

$$x^* = y^* + 2\log_{10}(1{\cdot}95y^* + 4{\cdot}10), \tag{2}$$

where

$$x^* = \log_{10}\left(\frac{\Delta p_p d^2}{4\rho\nu^2}\right) \quad \text{and} \quad y^* = \log_{10}\left(\frac{\tau_0 d^2}{4\rho\nu^2}\right).$$

In the Preston-tube Reynolds number range

$$1{\cdot}5 < y^* < 3{\cdot}5,$$

i.e.

$$5{\cdot}6 < U_\tau d/(2\nu) < 55,$$

the calibration is represented by the empirical relation

$$y^* = 0{\cdot}8287 - 0{\cdot}1381x^* + 0{\cdot}1437x^{*2} - 0{\cdot}0060x^{*3} \tag{3}$$

to within $\pm 1\frac{1}{2}$ % of τ_0.

Finally, in the region where

$$y^* < 1{\cdot}5,$$

i.e.

$$U_\tau d/(2\nu) < 5{\cdot}6,$$

the calibration results fall on a straight line

$$y^* = \tfrac{1}{2}x^* + 0{\cdot}037. \tag{4}$$

Present experiments with the tubes 1B to 4B also indicate that with a symmetrical bore for round Preston tubes the ratio of inside to outside diameter has a negligible effect on the calibration. This confirms the results of Rechenberg (1963).

In the following section, it is shown that the experimental calibration curve described above is compatible with that derived from the law of the wall using particular values of the constants A and B appearing in the logarithmic law and experimentally established Pitot displacement corrections.

4. Constants in the logarithmic law from the calibration curve

The validity of the law of the wall,

$$U/U_\tau = \mathrm{f}(U_\tau y/\nu) \tag{5}$$

is restricted to values of $U_\tau y/\nu$ less than some upper limit which we should expect to depend upon the type of flow, the pressure gradient and possibly the upstream history of the flow. Physical insight and dimensional reasoning have led to the definition of f in three parts, namely:

(*a*) a linear sublayer, where

$$U/U_\tau = U_\tau y/\nu; \tag{6}$$

(*b*) a fully turbulent region, where

$$U/U_\tau = A\log_{10}(U_\tau y/\nu) + B; \tag{7}$$

and (*c*) a transition zone, where the velocity can be conveniently represented by

$$U/U_\tau = A\log_{10}(U_\tau y/\nu + C) + B. \tag{8}$$

The constants A, B and C are supposedly universal. Accurate measurements in the first and last regions are comparatively rare, but the fully turbulent region of the flow has been explored by a large number of investigators. In pipe flows, as well as in boundary layers with moderate pressure gradients, the form of equation (7) is universally accepted, but there is no general agreement on the precise values of the constants A and B and their dependence, if any, on experimental conditions. In what follows we shall determine the values of A and B required to give agreement with the Preston-tube calibration curve described above. To do this we must consider the displacement effect of Pitot tubes resting on the wall. If the effective centre of a round Pitot tube, with external diameter d, is at $y = \frac{1}{2}Kd$, and the tube is fully submerged in the similarity region defined by equation (5), dimensional considerations lead to the conclusion that

$$K = K(U_\tau d/\nu) \quad \text{only.} \tag{9}$$

The form of this relationship has been determined experimentally by McMillan (1957). By the definition of the effective centre, therefore, the velocity recorded by a Preston tube, U_p, is the true velocity at $y = \frac{1}{2}Kd$. Thus,

$$\Delta p_p = \tfrac{1}{2}\rho U_p^2 = \tfrac{1}{2}\rho\,(U^2)_{y=\frac{1}{2}dK}. \tag{10}$$

From the above, it is now possible to construct the Preston-tube calibration curve in three parts.

(a) In the linear sublayer, equations (6) and (10) give

$$\Delta p_p = \tfrac{1}{2}\rho(U_\tau^2/\nu\,.\,\tfrac{1}{2}Kd)^2.$$

Therefore,

$$\log_{10}\left(\frac{\Delta p_p d^2}{4\rho\nu^2}\right) = 2\log_{10}\left(\frac{\tau_0 d^2}{4\rho\nu^2}\right) + \log_{10}(\tfrac{1}{2}K^2), \tag{11}$$

or

$$y^* = \tfrac{1}{2}x^* - \tfrac{1}{2}\log_{10}(\tfrac{1}{2}K^2). \tag{11a}$$

If the sublayer extends up to $U_\tau y/\nu = 5$, say, equation (11) will be valid in the range $y^* < 1{\cdot}4$.

(b) Similarly, in the transition zone, equations (8) and (10) lead to

$$x^* = y^* + 2\log_{10}\left\{\frac{A}{\sqrt{2}}\log_{10}(K10^{\frac{1}{2}y^*} + C) + \frac{B}{\sqrt{2}}\right\}. \tag{12}$$

The validity of (7) in the range $5 < U_\tau y/\nu < 60$ implies that equation (12) refers to the range $1{\cdot}4 < y^* < 3{\cdot}56$.

(c) Finally, in the fully turbulent part of the wall region, from equations (7) and (10) we have,

$$x^* = y^* + 2\log_{10}\left\{\frac{A}{2\sqrt{2}}(y^* + 2\log_{10}K) + \frac{B}{\sqrt{2}}\right\}, \tag{13}$$

for the range $3{\cdot}56 < y^*$.

Equations (11), (12) and (13) may be regarded as representing the Preston-tube calibration curve derived from the law of the wall, and by comparing them with the corresponding empirically determined equations (4), (3) and (2), the values of the constants A, B and C can be determined using McMillan's relationship for the displacement of the effective centre of the Pitot from its geometric centre.

Following this procedure for the fully turbulent region we obtain $A = 5{\cdot}5$ and $B = 5{\cdot}45$,† values which give excellent agreement with the measured velocity profiles shown in figure 2, one of which was obtained in the pipe and the other in a zero-pressure-gradient turbulent boundary layer (see § 7). This independent confirmation of the values obtained from the calibration curve greatly increases confidence in their accuracy; they are in fact very close to the values 5·5, 5·4 obtained by Sarnecki (1959) from a re-analysis of a very large number of published measurements.

In the transition zone characterized by $1{\cdot}5 < y^* < 3{\cdot}5$, it is possible to represent the experimental calibration in the form suggested by equation (12) with A and B values given above. In the absence of well-defined limits on the region in which velocity law (8) is valid, the value of C is rather difficult to determine, and the alternative approach of fitting a cubic, equation (3), has been preferred.

In the sublayer region, compatibility of equation (11) with experiment, equation (4), requires the value of K to be 1·30. Hence, if $\bar{\delta}$ is the displacement of the effective centre of the Pitot from its geometric centre towards the region of higher velocity, $\bar{\delta} = 0{\cdot}15d$. This value of $\bar{\delta}$ is precisely that determined by McMillan.

The fact that the Preston-tube calibration is virtually independent of the internal to external diameter ratio suggests that the Pitot displacement effect is mainly a function of the external diameter. Measurements by Rechenberg (1963) confirm this conclusion but show that the calibration may change appreciably for diameter ratios less than 0·2. In the present experiments, however, the tube $4B$ with a diameter ratio of 0·17 did not show any large-scale departures from the calibration curve.

5. Discussion

The present investigation goes some way towards explaining the discrepancy between Preston's original calibration in pipe flow and the flat-plate results obtained by the staff of the National Physical Laboratory (1958). The rather large disagreement between the two sets of measurements is at least partly due to what appears to be an error in Preston's original calibration, but some anomalies still remain unexplained. Smith & Walker (1958) suggest that the constants A and B in the logarithmic law are different in pipe flow and boundary layers, and that their numerical values are dependent on Reynolds number. Head & Rechenberg, on the other hand, have provided quite conclusive evidence in favour of complete similarity of the law of the wall in the two cases. The relation between the inner law, Pitot displacement effects and Preston-tube calibration curve has been outlined in § 4. It is seen that the calibration curve in the range $y^* > 3{\cdot}56$ corresponds to only one set of values of the constants A and B. It is difficult to see therefore how the two very different inner-law measurements of Smith & Walker (1958) and Bradshaw & Gregory (1961) (or the National Physical Laboratory (1958)) should be in excellent agreement as regards the Preston-tube calibration; in spite of the fact that both sets of measurements were

† Strictly speaking, the values of A and B so determined would be slightly in error since McMillan's corrections do not take into account the effect of turbulence on Pitot tubes.

made in zero-pressure-gradient flat-plate boundary layers at similar Reynolds numbers, the constants given by Smith & Walker ($A = 5{\cdot}0$, $B = 7{\cdot}15$) and the Staff of the National Physical Laboratory ($A = 4{\cdot}9$, $B = 5{\cdot}9$) are very different. Disagreement of this scale can only come from inaccuracies in the measurement of τ_0 and/or failure to take account of Pitot displacement corrections. Landweber (1960) has re-analysed Smith & Walker's velocity measurements using McMillan's displacement corrections and turbulence corrections and shown that the true values of A and B must be different from those quoted by the authors. Constants derived from the profiles corrected by Landweber are in fact in good agreement with the values 5·5 and 5·45 suggested here.

Thus, the effect of the wall on velocity-measuring devices can be large, and since different experimenters use different corrections or none at all, some of the disagreement in the log-law constants can be attributed to these. Surveys of velocity profiles carried out by Sarnecki (1959) and Kestin & Richardson (1963), and others, show that even though the data are scattered over a fairly wide range of A and B, the values 5·5 and 5·45 can be used to represent the pipe and boundary-layer profiles adequately. Since the present calibration curve is compatible with constants $A = 5{\cdot}5$ and $B = 5{\cdot}45$ in the logarithmic region of the law of the wall it can be used to determine skin friction in boundary layers. The experiments of Head & Rechenberg lend support to these observations.

Finally, it is worth mentioning that the experimental calibration of Preston tubes in pipe flow, figure 4, extends up to $U_\tau d/\nu$ values of 1270. This suggests that the logarithmic portion in the law of the wall extends at least up to $U_\tau y/\nu$ values of 635. In zero-pressure-gradient boundary layers the region of universality is expected to be dependent on Reynolds number. Experiments of Smith & Walker (1958) suggest that the law of the wall is valid in the region $y/\delta < \frac{1}{6}$ where δ is the boundary-layer thickness. In practice, therefore, it is worth checking the result of a large Preston tube against a smaller one, to make sure that the larger tube is in fact within this region.

6. Preston tubes in pressure gradients

So far we have considered the calibration of the Preston tube and the universality of the law of the wall on the assumption that such pressure gradients as exist in fully developed pipe flow at high Reynolds numbers have a negligible effect on the velocity distribution in the wall region, an assumption fully supported by the fact that the results from different sizes of Preston tubes and different pipe Reynolds numbers give a unique calibration curve. For sufficiently severe pressure gradients however it is certain that the inner law in its usual form must break down and the Preston-tube calibration would be expected to change. It is the object of this part of the paper to establish the limits of pressure gradient, both favourable and unfavourable, within which the calibration curve given in figure 4 is valid for practical purposes. It was at first thought that this would be a relatively straightforward procedure but the initial experiments described below gave somewhat unexpected results which led to a rather more comprehensive investigation than was at first intended; part of the remainder of this report is therefore devoted to a discussion of detailed velocity measurements in the wall region of boundary-layer flows with severe pressure gradients.

Before describing the experiments it is convenient to define a pressure-gradient parameter which measures the severity of the pressure gradient as it affects the flow in the wall region. Such a parameter based on the relevant variables in this region can readily be obtained by dimensional analysis; it is $\nu/(\rho U_\tau^3).dp/dx$ (where p is the static pressure and x the streamwise co-ordinate), which we shall denote by the symbol Δ. The significance of this parameter has been remarked upon by Rotta (1962), Mellor (1964) and others.

The first set of experiments was conducted on the plane wall of a wind tunnel with a flexible opposite wall which could be adjusted to give any desired pressure distribution. The experimental arrangement is shown in figure 6(*a*) from which it will be seen that a sublayer fence was mounted in the surface with a Preston

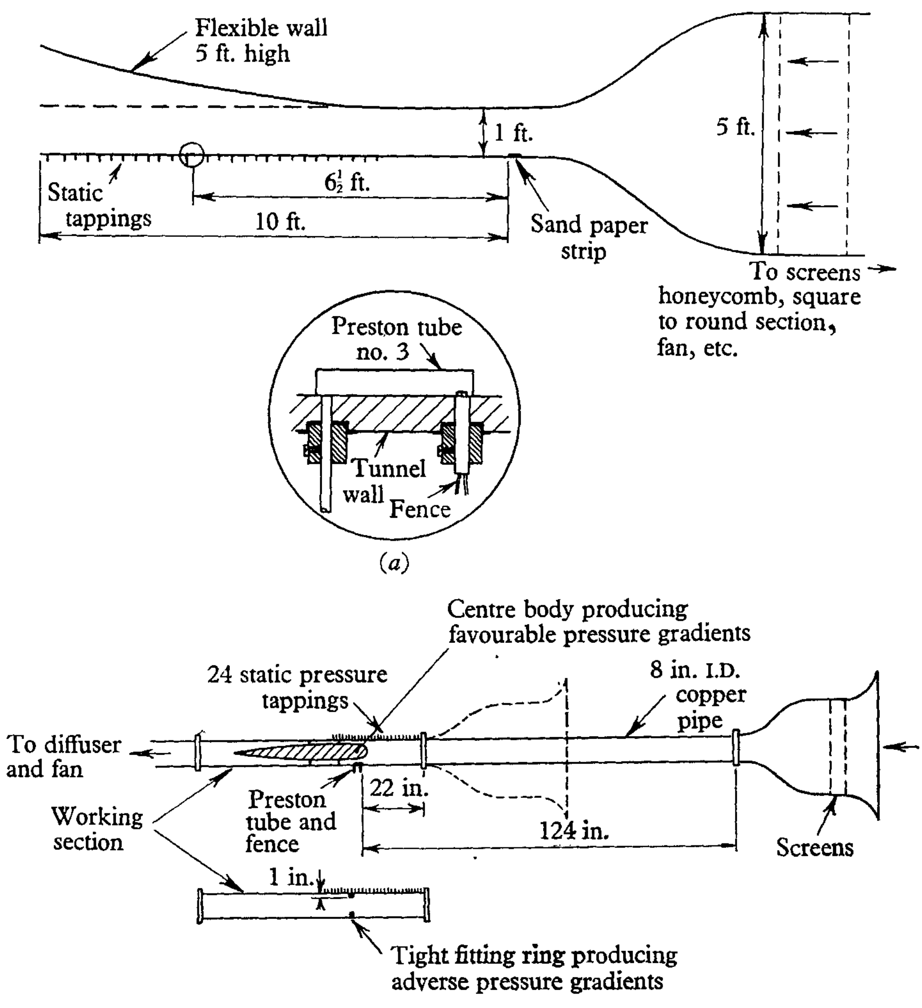

For legend see facing page.

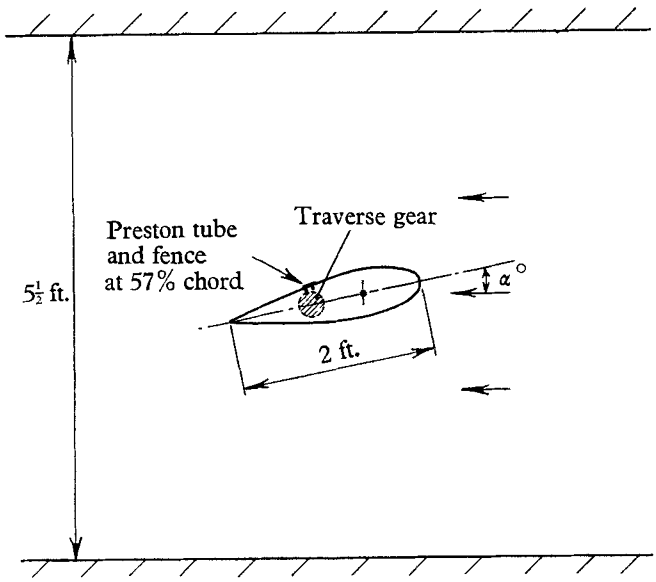

(c)

FIGURE 6. (a) Experimental arrangement for tests with pressure gradients in the 5 ft. × 1 ft. blower tunnel. (b) Experimental arrangement for tests with pressure gradients in the 8 in. diameter pipe. (c) Experimental arrangement for tests with pressure gradients. A 23·4 % thick wing section mounted vertically in a 4 ft. × $5\frac{1}{2}$ ft. working section of the return circuit wind tunnel.

tube fitted over it, the reading of the Preston tube being unaffected by the presence of the fence, and that of the fence being unaffected by the Preston tube when this was pushed away from the wall. Corresponding readings of Preston tube and fence were taken over a range of speeds with both zero pressure gradient and with arbitrary pressure gradients imposed. If the readings of both devices were unaffected by pressure gradients then of course the plots of Preston-tube readings against fence readings would have lain on a single curve, but in fact quite wide divergences were obtained for non-zero pressure gradients. Typical results are shown in figure 7. In assessing the significance of these curves it need not be assumed that the fence readings are unaffected by pressure gradient but only that they are affected to a much smaller extent than the corresponding Preston-tube readings. It will be seen that in both favourable and adverse pressure gradients the Preston tube tended to overestimate the skin friction (i.e. for a given fence reading the Preston-tube reading was greater than for zero-pressure-gradient conditions). Moreover in given favourable pressure-gradient conditions the error actually increased with decreasing Preston-tube diameter. This behaviour was quite unexpected and it appeared that the explanation could be found only by detailed measurements of velocity in the wall region.

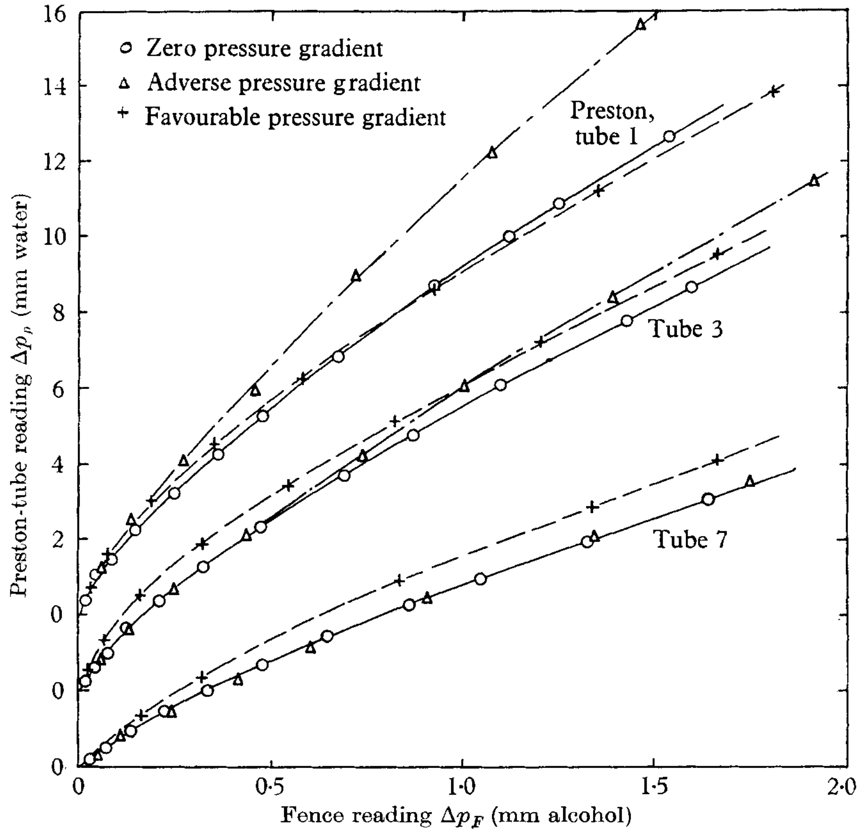

FIGURE 7. A direct comparison between fence and Preston-tube measurements in pressure gradients.

7. Measurements of velocity distributions in the wall region with pressure gradients

To plot velocity distributions in the wall region in the conventional way it was necessary to determine the value of the friction velocity U_τ with reasonable accuracy. To do this the sublayer fence was calibrated in zero pressure gradient by using Preston tubes of different diameters and the calibration curve of figure 4. The fact that eight different tubes ranging in diameter from 0·0285 to 0·75 in. gave the same skin friction value to within $\pm 1\,\%$ provided additional evidence for the substantial identity of the velocity distribution in the wall region of pipe and boundary-layer flows. Preliminary calculations of the velocity distribution in the sublayer indicated that in strong pressure gradients the reading of the fence might be appreciably in error, and the procedure described in appendix 1 was used to determine the corrections. These have been applied in all the measurements described below and amounted to about $1\frac{1}{2}\,\%$ of τ_0 at low values of Δ to $8\,\%$ of τ_0 at the highest value of Δ encountered in the experiments, and are much smaller than the corresponding errors in the Preston-tube readings. A typical zero-pressure-gradient boundary-layer profile (obtained using a flattened Pitot) has been plotted in figure 2.

The first measurements of velocity distributions were made using the same experimental arrangements as described in the previous section, a circular Pitot tube of 0·054 in. diameter being traversed through the boundary layer. Typical measurements, with corrections applied for displacement of the effective centre of the Pitot, are shown in figure 8. It will be seen that the results adequately account for the errors in Preston-tube readings described in the previous section. The profiles show that, in adverse pressure gradients, Preston tubes of increasing diameter register progressively larger errors due to the early departure of the velocity distribution from the usual logarithmic law. In favourable gradients of sufficient magnitude it is evident that there is no conformity with this law and

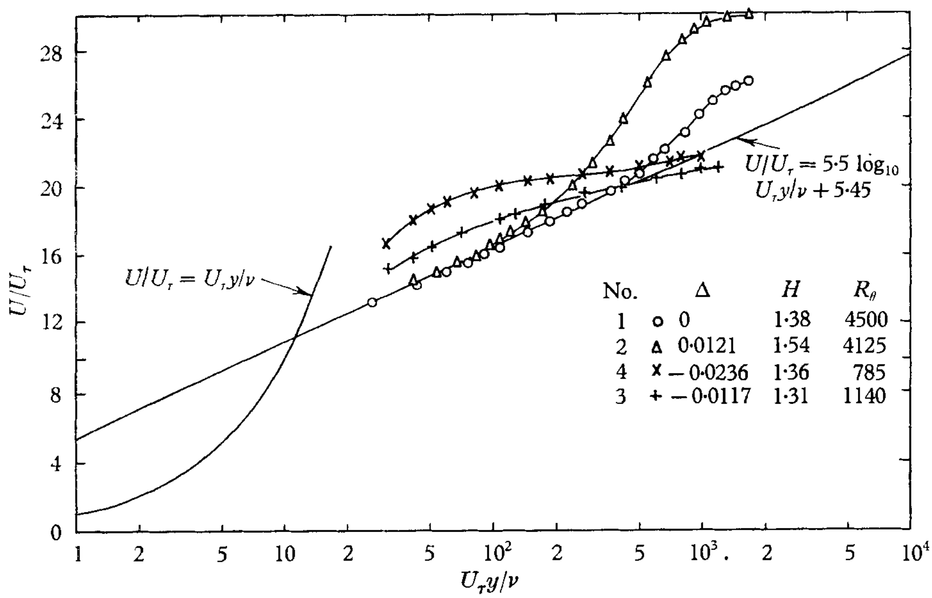

FIGURE 8. Velocity profiles on the flat plate of the blower tunnel. ○, Zero pressure gradient; △, mild adverse gradient and x; +, favourable gradients.

that a Preston tube of small diameter will give a large overestimate, while a larger tube will fortuitously give a nearly correct reading. It is reasonable to suppose that the complete departure from the usual inner law which is observed represents the process of reversion to laminar flow and it was thought that this might be associated with the low boundary-layer Reynolds numbers obtained in these conditions. To achieve a high boundary-layer Reynolds number with a strong favourable gradient it was decided to carry out experiments in the entry length of the 8 in. diameter pipe introducing a highly favourable pressure gradient at some distance downstream by the presence of a centre body. The effect of adverse pressure gradients could also be studied by fitting a ring in place of the centre body as shown in figure 6(*b*) and described by Head & Rechenberg (1962).

Pipe experiments

A skin-friction fence was fitted in the working section of the 8 in. pipe and calibrated in fully developed flow. The entry length was then shortened to give axisymmetric boundary-layer flow with transition fixed at the end of a bell-mouthed entry by means of a serrated ring. Velocity profiles in the wall region measured at various mean speeds and with entry lengths of 124 in. and 22 in. agreed with those in fully developed pipe flow and the zero-pressure-gradient boundary layer.

As mentioned above, favourable pressure gradients were obtained by mounting a 44 in. long centre body in the pipe. It consisted of a 6 in. diameter, 12 in. long cylinder with a paraboloid nose 8 in. in length and a conical tail. The body was supported in the pipe by means of six piano wires in tension and could be fitted in different positions relative to the measuring station. Figure 6 (*b*) shows the general layout of the apparatus. Velocity profiles, skin friction (i.e. fence readings) and static pressure distributions along the pipe were measured with the two entry lengths and various free-stream velocities for different relative positions of the centre body and measuring station. Some of the profiles are shown in figure 9. The static-pressure variation across the pipe boundary layer was found to be negligible.

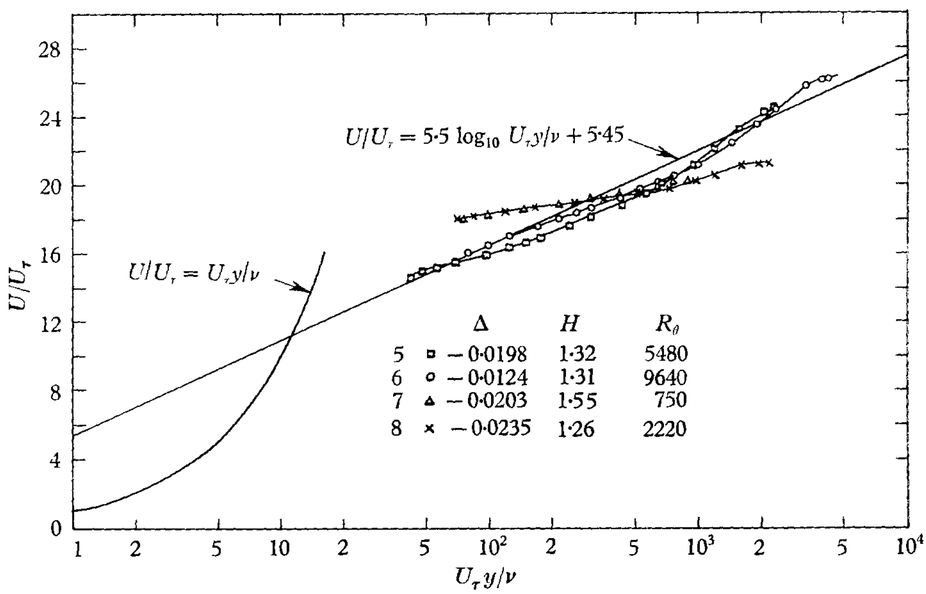

FIGURE 9. Centre body in pipe. Favourable pressure gradient profiles.

Adverse pressure gradients were produced by the ring described by Head & Rechenberg. Velocity profiles were measured with different ring positions relative to the measuring station, different free-stream velocities and the two entry lengths. Two representative profiles are shown in figure 10.

Aerofoil experiments

To obtain velocity profiles close to separation, a symmetrical aerofoil with 2 ft. chord, 4 ft. span and maximum thickness-to-chord ratio of 0·234 at 30 % chord was mounted in a $5\frac{1}{2}$ ft. by 4 ft. working section wind-tunnel. The experimental arrangement is shown in figure 6 (*c*). The traverse gear used to measure velocity profiles was built into the aerofoil so as to avoid flow distortion. Transition was fixed at 5 % chord by means of a 0·040 in. diameter wire. Velocity traverses were made at various incidences ($-2° < \alpha < 8{\cdot}7°$) and approximately constant tunnel Reynolds number. Some of these profiles are shown in figure 10. The separation point (as detected by null reading of the fence) moved past the measuring station at an incidence of 9·3°; above 8·7° however accurate measurement of mean velocity profiles became excessively difficult due to large-scale fluctuations.

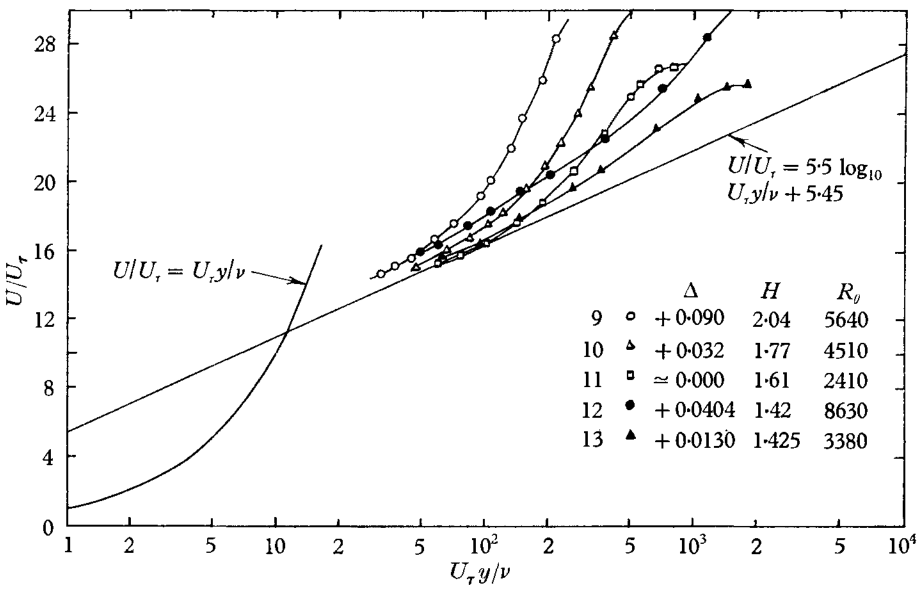

FIGURE 10. Adverse pressure-gradient profiles. ●, ▲, Pipe experiments with ring; ○, △, □, aerofoil experiments.

8. Results and discussion

Since the experiments just described were carried out to investigate the flow in the wall region, no attempt was made to measure the overall development of the boundary layers. The influence of the upstream history of the layer cannot therefore be readily assessed. However, the results show unmistakably that large departures from the usual law of the wall occur in the presence of severe pressure gradients. A detailed discussion of velocity distribution in the layer is beyond the scope of the present paper, and only a few representative results are shown in figures 8, 9 and 10 to indicate the general trends. The values of the pressure-gradient parameter Δ and the usual overall characteristics of the boundary layer, H and R_θ, are also quoted. It was thought initially that the usefulness of Preston tubes might be extended if the pressure-gradient flows showed some kind of similarity. Thus, if it could be shown that the flow in the wall region could be represented by

$$U/U_\tau = f(U_\tau y/\nu, \Delta),$$

a single parametric family of calibration curves, dependent on Δ, could be obtained. It appears from the present results that while the numerical value of

Δ gives some indication of the state of the flow it certainly does not define a unique velocity distribution. Townsend (1962), in his analysis of linear-stress equilibrium layers, shows in fact that the essential parameter describing the velocity variation in the fully turbulent part of the layer is the slope of the shear stress profile, α. Thus,

$$U/U_\tau = \mathrm{f}\,(U_\tau y/\nu, \alpha\nu/(\rho U_\tau^3)), \tag{14}$$

where α is a function of the pressure gradient and the local flow accelerations. This therefore rules out the existence of similarity conditions based on the pressure-gradient parameter Δ.

The present experiments indicate that in both adverse and favourable pressure gradients the departure of the velocity distribution from the law of the wall, in the initial stages, is gradual. In the former case this gradual departure is more obvious. Comparison of adverse pressure-gradient profiles 1 and 2 in figure 8 with the constant-pressure boundary-layer profile in figure 2 shows that the application of pressure gradients reduces the extent of the region in which the law of the wall is valid. This process continues until at some value of Δ higher than those of profiles 1 and 2, the straight line portion is absent altogether. The general trend is also shown by the large Δ profiles of figure 10.

In favourable pressure gradients the picture is slightly different. Initially, when $|\Delta|$ values are small, the departure from the logarithmic law is in the opposite direction to that in adverse pressure gradients (e.g. profiles 5 and 6 in figure 9). As $|\Delta|$ increases, the departure starts at decreasing values of $U_\tau y/\nu$, until at some limiting value of Δ, depending on the flow geometry, the fully-turbulent region of the inner layer no longer exists. The profiles then fall above the straight line and show greater discrepancies with the straight line at lower values of $U_\tau y/\nu$. This is seen from profiles corresponding to high negative values of Δ in figures 8 and 9. These profiles closely resemble those measured by Schlinger & Sage (1953) in laminar-to-turbulent transition regions of fully-developed channel flow, and therefore, it is thought, characterize a reverse transition process.

At present, it appears that very little is known about the conditions in which a turbulent boundary layer reverts to the laminar state though this process is known to occur with high rates of suction in zero pressure gradient (Sarnecki 1959) or in sufficiently favourable pressure gradients on a solid surface (Sergienko & Gretsov 1959). In pipe flow, a progressive reduction in Reynolds number is accompanied by an increasingly negative value of the pressure-gradient parameter Δ. In fact it can be simply shown that if the Blasius turbulent skin friction law

$$C_f = 0{\cdot}079 R^{-\frac{1}{4}}, \tag{15}$$

where C_f is the skin-friction coefficient and R the Reynolds number based on pipe diameter and mean velocity, is assumed, then

$$\Delta = -20{\cdot}1 R^{-\frac{7}{8}}. \tag{16}$$

It is worth noting that if the Reynolds number for reverse transition in pipe flow is taken as 3000, the corresponding value of $-\Delta$ is 0·018, which is generally similar to the values noted for major departures from the inner-law velocity distribution in boundary-layer flow. There is thus the possibility that reversion from turbulent to laminar flow occurs in a pipe rather as a result of effectively increasing favourable pressure gradient than of reduction in Reynolds number as such. This question is at present being further explored.

Having examined the circumstances in which the departures from the law of the wall are such as to completely invalidate the use of the Preston tube we now consider the limits which must be imposed on pressure gradients if the skin friction is to be measured with some specified degree of accuracy. We have already seen that the departure of the wall region velocity distribution from the inner law is gradual and small for small values of Δ. The Preston tube would therefore incur a small error which depends on its diameter and the value of Δ. By the method outlined in §4 it is possible to estimate this error if the tube Reynolds number, $U_\tau d/\nu$, and the actual velocity distribution in the wall region are known. After a critical examination of some 76 velocity profiles in adverse and favourable pressure gradients the following limiting values of Δ are suggested if Preston tubes are to record τ_0 within the prescribed error range.

(i) Adverse pressure gradients—

$$\text{maximum error } 3\,\%\text{: } 0 < \Delta < 0{\cdot}01,\ U_\tau d/\nu \leqslant 200;$$
$$\text{maximum error } 6\,\%\text{: } 0 < \Delta < 0{\cdot}015,\ U_\tau d/\nu \leqslant 250.$$

(ii) Favourable pressure gradients—

$$\text{maximum error } 3\,\%\text{: } 0 > \Delta > -0{\cdot}005,\ U_\tau d/\nu \leqslant 200,\ d/dx(\Delta) < 0;$$
$$\text{maximum error } 6\,\%\text{: } 0 > \Delta > -0{\cdot}007,\ U_\tau d/\nu \leqslant 200, d/dx(\Delta) < 0.$$

These limiting conditions are purely empirical in nature and are quoted as a rough guide to the user of Preston tubes. The additional restriction of $d\Delta/dx < 0$ in favourable gradients has been imposed to ensure that the flow is sufficiently far from the commencement of laminar reversion.

In view of the fact that the flow in the wall region is not uniquely defined by the parameter Δ the limiting values quoted above must be used with caution. In incompressible, fully developed pipe flow, Δ (and therefore pipe Reynolds number, equation (16)) completely specifies the state of the flow. The lower limit of the Reynolds number corresponding to $\Delta = -0{\cdot}005$ of the 3 % criterion, from equation (16), is approximately 13000. Thus for Reynolds numbers lower than this value, the law of the wall in pipe flows may show discrepancies larger than 3 % of τ_0. This may account for some scatter in the experimental data of Preston-tube calibration in the $\frac{1}{2}$ in. diameter pipe. The 8 in. and 2 in. diameter pipe experiments are well within the 3 % error range.

It is interesting to compare the present results with those of other experimenters. Ludwieg & Tillmann's (1950) experiments are usually quoted in support of universality of the law of the wall in pressure gradients. These measurements were carried out within the range $-0{\cdot}002 < \Delta < 0{\cdot}00575$, and therefore do not show any large-scale disagreement with the law of the wall. Similarly, Fage's (1938) aerofoil results give a unique inner law within the limits of experimental scatter, since the maximum value of Δ obtained was 0·0060. In Schubauer & Klebanoff's (1951) experiments the velocity profiles begin to diverge from the law of the wall around the 22 ft. station. The value of Δ corresponding to this station was approximately 0·007; skin friction was estimated by the method of Clauser (1954). The measurements made after this station compare favourably with Stratford's (1959) zero-shear-stress layer velocity distribution (see Townsend 1961). The present experiments also confirm the observations of Bradshaw & Gee (1959) who found that in both adverse and favourable pressure gradients the use of Preston's calibration curve predicted values of τ_0 which were too high. In their experiments the pressure-gradient parameter range was approximately $0{\cdot}0055 < \Delta < 0{\cdot}0117$ and $-0{\cdot}0036 < \Delta < -0{\cdot}0022$. The disagreement between Stanton-tube and Preston-tube results was much larger in the favourable gradients.

9. Conclusions

A calibration curve for the Preston tube is presented which is in excellent agreement with that given by Rechenberg (1963) and Head & Rechenberg (1962) and differs appreciably from the original calibration given by Preston (1954). From the calibration curve it has been possible to determine, by the use of McMillan's (1957) corrections for the displacement of the effective centre of a Pitot resting on the wall, the values of the constants A and B appearing in the logarithmic region of the law of the wall. The values obtained ($A = 5{\cdot}5$, $B = 5{\cdot}45$) gave excellent agreement with measured velocity distributions in the wall region of both pipe and boundary-layer flows, and are close to those proposed by Sarnecki (1959).

In severe favourable and adverse pressure gradients the Preston tube was found to overestimate the skin friction. Detailed measurements of velocity in the wall region showed that large deviations from the law of the wall occurred in both favourable and adverse pressure gradients, those in the former case being much more severe and evidently associated with the onset of reverse transition.

The value of the pressure-gradient parameter $\nu/(\rho U_\tau^3)\,.\,dp/dx$ was not found to define the flow in the wall region completely, but it has nevertheless been possible to assign tentative limits in terms of this parameter within which the Preston tube can be used with acceptable accuracy.

The author wishes to acknowledge gratefully the assistance and constant encouragement he has received from Prof. W. A. Mair and Dr M. R. Head during the course of this work.

Appendix 1

The effect of pressure gradients on the skin friction fence

The following represents an attempt to estimate the correction to be applied to fence readings in presence of pressure gradients. If it is assumed that the fence is fully submerged in the sublayer and that the local flow is substantially laminar then the shear-stress relation

$$\tau_0 = \rho\nu \left.\frac{\partial U}{\partial y}\right|_0 \tag{A 1}$$

and the wall boundary condition

$$\partial\tau/\partial y = dp/dx, \tag{A 2}$$

lead to the velocity distribution

$$U = (\tau_0/\rho\nu)\,y + (1/2\rho\nu)\,(dp/dx)\,y^2 + \ldots, \tag{A 3}$$

or

$$U/U_\tau = (U_\tau y/\nu) + \tfrac{1}{2}\Delta(U_\tau y/\nu)^2 + \ldots. \tag{A 3a}$$

For zero pressure gradient, equation (A 3a) reduces to the usual linear sub-layer law. For small (compared with unity) values of $\frac{1}{2}\Delta . U_\tau y/\nu$ we include only the first two terms in the series expansion.

The sketch below shows the velocity profiles of equation (A 3) approaching a fence of height h.

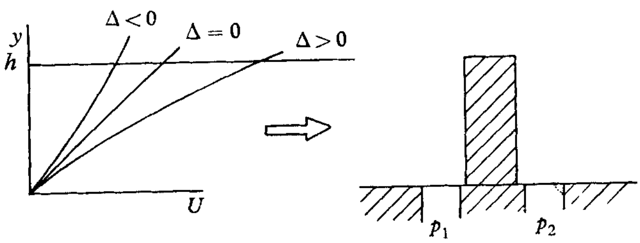

It is not unreasonable to suppose that the pressure difference recorded across the fence depends upon the velocity distribution in the region $0 < y < h$ and not on the value of τ_0 as such. As a first and crude approximation, if it is assumed that the reading of the fence is proportional to the square of the mean velocity, U_m, over the face of the fence, we have

$$(p_1 - p_2)/\tfrac{1}{2}\rho U_m^2 = \text{const.}, \tag{A 4}$$

and using equation (A 3) to evaluate U_m, we obtain the correction formula,

$$\begin{aligned}(p_1 - p_2)_{\Delta \neq 0} &= (p_1 - p_2)_{\Delta=0}\{1 + \tfrac{1}{3}\Delta(U_\tau h/\nu)\}^2, \\ &\simeq (p_1 - p_2)_{\Delta=0}(1 + 0{\cdot}67\Delta(U_\tau h/\nu)),\end{aligned} \tag{A 5}$$

$(p_1 - p_2)_{\Delta \neq 0}$ is the fence reading in pressure gradients, τ_0 is the true wall shear stress and $(p_1 - p_2)_{\Delta=0}$ is the corrected fence reading which corresponds to τ_0 through the zero-pressure-gradient fence calibration curve. Thus, when $(p_1 - p_2)_{\Delta \neq 0}$ and h are known, an iterative procedure can be used to determine τ_0.

In view of the drastic assumption implied by equation (A 4) the above correction is regarded as a first approximation. A more accurate assessment of the corrections could be obtained in the following manner. Consider the case where $\Delta = 0$ and the velocity distribution is linear. When the flow Reynolds number, $U_\tau h/\nu$, is of the order of unity, Stokes-flow analyses of Taylor (1938) and Thom (1952) show that the pressure recorded by a Stanton tube is proportional to τ_0, i.e.

$$(p_1 - p_2) \propto \tau_0 \propto U_c,$$

where U_c is a characteristic velocity, say the velocity at $y = y_1$. On the other hand, both Stanton tubes and Preston tubes at Reynolds numbers of the order of 30 show dependence of the form,

$$(p_1 - p_2) \propto \tau_0^2 \propto U_c^2.$$

Thus it is possible to take account of the variation in Reynolds number by writing

$$(p_1 - p_2) = a_1 \tau_0^b = a_2 U_c^b, \tag{A 6}$$

where the index b depends on Reynolds number and a_1 and a_2 are functions of ρ, ν and the characteristic height of the skin friction measuring device.

Equation (A 6) is compatible with the existing data on Stanton tubes. Zero-pressure-gradient (i.e. linear velocity-profile) analyses of Taylor (1938), Thom (1952) and Gadd (1960) and experimental calibrations of Trilling & Hakkinen (1955), Hool (1956), Bradshaw & Gregory (1959) and Smith, Gaudet & Winter (1964) can all be represented by

$$\frac{(p_1 - p_2) h^2}{\rho \nu^2} = A \left(\frac{\tau_0 h^2}{\rho \nu^2} \right)^b,$$

i.e.

$$(p_1 - p_2) = a_1 \tau_0^b.$$

The experimental value of b quoted by the various sources listed above ranges from Stokes-flow value of unity (Taylor and Thom) to 1·67 (Trilling & Hakkinen). Gadd obtained 1·33, Bradshaw & Gregory 1·50 and Hool 1·60.

Now, equation (A 6) would be expected to hold for the skin-friction fence as well. The three sets of fence calibration data obtained in the present experiments, i.e. in the 8 in. diameter pipe, on the flat plate, and on the aerofoil, accurately confirm the validity of (A 6). The Reynolds number range covered by these calibrations was $4 < U_\tau h/\nu < 8$ approximately and the value of b was found to be $1{\cdot}47 \pm 0{\cdot}07$. Thus for the zero-pressure-gradient fence calibration we write

$$(p_1 - p_2) = \text{const.} \times \tau_0^{1\cdot 5}. \tag{A 7}$$

In the presence of pressure gradients the fence reading would be expected to depend on the velocity distribution in the region $0 < y < h$ and not on τ_0 as such. Because of the linear profile in zero pressure gradient, in equation (A 7) any velocity may be taken as characteristic of the fence region but no such freedom of choice is available when $\Delta \neq 0$, and the velocity distribution is given by equation (A 3). In the absence of detailed experimental data, the choice of a velocity representative of the region $0 < y < h$ must be largely arbitrary. Physically, it would seem likely that the true correction to be applied to the fence reading would be less than that resulting from the use of $U_c = U$ at $y = h$, which is,

$$\left. \begin{aligned} (p_1 - p_2)_{\Delta \neq 0} &= (p_1 - p_2)_{\Delta = 0} \{1 + \tfrac{1}{2}\Delta(U_\tau h/\nu)\}^{1\cdot 5} \\ &\simeq (p_1 - p_2)_{\Delta = 0} \{1 + 0{\cdot}75\, \Delta(U_\tau h/\nu)\}. \end{aligned} \right\} \tag{A 8}$$

The use of $U_c = U_m$, the mean velocity over the face of the fence, as in the first approximation, leads to

$$\left. \begin{aligned} (p_1 - p_2)_{\Delta \neq 0} &= (p_1 - p_2)_{\Delta = 0} \{1 + \tfrac{1}{3}\Delta(U_\tau h/\nu)\}^{1\cdot 5} \\ &\simeq (p_1 - p_2)_{\Delta = 0} \{1 + \tfrac{1}{2}\Delta(U_\tau h/\nu)\}. \end{aligned} \right\} \tag{A 9}$$

This should be an improvement on the original estimate of equation (A 5), in so far as U_m can be taken as the representative velocity.

In view of the fact that the fence corrections given by equations (A 5), (A 8) and (A 9) are all of the same order of magnitude and did not exceed 8 per cent of

τ_0 in the most severe pressure-gradient conditions encountered in the present experiments the choice of the numerical constant appearing in the correction formula is not considered to be too critical. In the case of the velocity profiles presented in the text the corrections have been applied according to the simpler estimate of equation (A 5).

These corrections, when applied to the measured velocity profiles, improved the agreement with the law of the wall in favourable pressure gradients and increased the disagreement in adverse gradients.

A small error is also introduced in the fence reading due to the finite stream-wise displacement of the two static tappings on either side of the fence. This correction was found to be negligibly small in the present experiments.

REFERENCES

Bradshaw, P. & Gee, M. T. 1959 Note on the inner velocity profiles of non-equilibrium turbulent boundary layers. *Aero. Res. Counc.* **20**, 889. (Unpublished.)

Bradshaw, P. & Gregory, N. 1958 Calibration of Preston tubes on a flat plate using measurements of local skin friction. *Aero. Res. Counc.* **20**, 199. (Unpublished.)

Bradshaw, P. & Gregory, N. 1959 The determination of local turbulent skin friction from observations in the viscous sublayer. *Aero. Res. Counc. R. & M.* no. 3202.

Clauser, F. H. 1954 Turbulent boundary layers in adverse pressure gradients. *J. Aero. Sci.* **21**, 91.

Fage, A. 1938 Profile and skin-friction aerofoil drags. *Aero. Res. Counc. R. & M.* no. 1852.

Gadd, G. E. 1960 A note on the theory of the Stanton tube. *Aero. Res. Counc. R. & M.* no. 3147.

Head, M. R. & Rechenberg, I. 1962 The Preston tube as a means of measuring skin friction. *J. Fluid Mech.* **14**, 1.

Hool, J. N. 1956 Measurements of skin friction using surface tubes. *Aircraft Engineering*, **28**, 52.

Kestin, J. & Richardson, P. D. 1963 Heat transfer across turbulent incompressible boundary layers. *J. Heat and Mass Transfer*, **6**, 147.

Landweber, L. 1960 Reanalysis of boundary-layer data on a flat plate. Written discussion of Ninth International Towing Tank Conference, Paris, 1960. Iowa Institute of Hydraulic Research, State University of Iowa.

Ludwieg, H. & Tillmann, W. 1950 Investigation of the wall shearing stress in turbulent boundary layers. (Trans.) *NACA TM* no. 1285.

McMillan, F. A. 1957 Experiments on Pitot tubes in shear flow. *Aero. Res. Counc. R. & M.* no. 3028.

Mellor, G. L. 1964 Equilibrium turbulent boundary layers. *Tech. Note. AIAA J.* **2**, 1650.

Preston, J. H. 1954 The determination of turbulent skin friction by means of Pitot tubes. *J. Roy. Aero. Soc.* **58**, 109.

Rechenberg, I. 1963 Messung der turbulenten Wandschubspannung. *A. Flugwiss*, **11**, 429.

Rotta, J. C. 1962 Turbulent boundary layers in incompressible flow. *Progress in Aeronautical Sciences*, **2**, 72. London: Pergamon Press.

Sarnecki, A. J. 1959 The turbulent boundary layer on a permeable surface. Ph.D. Thesis, Cambridge University.

Schlinger, W. G. & Sage, B. H. 1953 Velocity distribution between parallel plates. *Ind. Eng. Chem.* **45**, 2636.

SCHUBAUER, G. B. & KLEBANOFF, P. S. 1951 Investigation of separation of the turbulent boundary layer. *NACA Rep.* no. 1030.

SERGIENKO, A. A. & GRETSOV, V. K. 1959 Transition from a turbulent to a laminar boundary layer. (Trans.) *RAE Trans.* no. 827.

SMITH, K. G., GAUDET, L. & WINTER, K. G. 1964 The use of surface Pitot tubes as skin-friction meters at supersonic speeds. *Aero. Res. Counc. R. & M.* no. 3361.

SMITH, D. S. & WALKER, J. H. 1958 Skin friction measurements in incompressible flow. *NACA TN*, no. 4231.

STAFF OF THE AERODYNAMICS DIVISION, N. P. L. 1958 On the measurement of local surface friction on a flat plate by means of Preston tubes. *Aero. Res. Counc. R. & M.* no. 3185.

STRATFORD, B. S. 1959 An experimental flow with zero skin-friction throughout its region of pressure rise. *J. Fluid Mech.* **5**, 17.

TAYLOR, G. I. 1938 Measurements with a half Pitot tube. *Proc. Roy. Soc.* A, **166**, 476.

THOM, A. 1952 The flow at the mouth of a Stanton tube. *Aero. Res. Counc. R. & M.* no. 2984.

TOWNSEND, A. A. 1961 Equilibrium layers and wall turbulence. *J. Fluid Mech.* **11**, 97.

TOWNSEND, A. A. 1962 The behaviour of a turbulent boundary layer near separation. *J. Fluid Mech.* **12**, 536.

TRILLING, L. & HAKKINEN, R. J. 1955 The calibration of the Stanton tube as a skin-friction meter. 50 *Jahre Grenzschichtforschung*, p. 201. Braunschweig: Friedr. Vieweg und Sohn.